IEEE Access
Multidisciplinary | Rapid Review | Open Access Journal

Received July 26, 2020, accepted August 22, 2020, date of publication August 31, 2020, date of current version September 18, 2020.

Digital Object Identifier 10.1109/ACCESS.2020.3020618

Uplink Reference Signals for Energy-Efficient Handover

MUHAMMAD TAYYAB[1,2], GEORGE P. KOUDOURIDIS[3], XAVIER GELABERT[3], AND RIKU JÄNTTI[2], (Senior Member, IEEE)

[1]Huawei Technologies Oy (Finland) Company Ltd., FI-00180 Helsinki, Finland
[2]Department of Communications and Networking, School of Electrical Engineering, Aalto University, FI-00076 Espoo, Finland
[3]Huawei Technologies Sweden AB, SE-164 94 Kista, Sweden

Corresponding author: Muhammad Tayyab (muhammad.tayyab@aalto.fi)

This work was supported by the European Union's H2020 Research and Innovation Program under Grant H2020-MCSA-ITN- 2016-SECRET 722424 [43].

ABSTRACT The ever-growing data rate demand from cellular users increases the associated power consumption that directly contributes to the global warming of the environment. Also, achieving high system capacity by increasing the density of the base stations (BSs) increases the number of handovers (HOs) which for moderate-to-high-speed users implies significant signaling traffic overhead. One of the key research objectives of this paper is to identify the different signaling overheads occurring during the HO procedure in current 3GPP cellular networks (e.g. Long Term Evolution (LTE)/ New Radio (NR)) and, among those, which are the main contributors to power consumption. Specifically, we analyze the impact of signaling messages transmitted and received during HO on the power consumption for both the BS and the User Equipment (UE). System-level simulations are performed for a detailed quantitative analysis. Our analysis shows that the transmission of the measurement reports is the largest contributor to air-interface signaling and that its contributed total power consumption is higher than the random access channel (RACH) signaling and the signaling confirming the HO. To eliminate measurement reports and effectively reduce the power consumption associated with the HO in future networks, we propose a HO procedure that exploits uplink (UL) reference signals (RSs), namely the sounding reference signal (SRS), transmitted by UEs. The numerical results show that the proposed SRS-based method reduces the total power consumption during the HO procedure by 30% in comparison to the legacy downlink RS based measurement method in current cellular networks. Also, this method improves the UE battery lifetime by reducing the RS transmissions and measurements significantly, UE transmitted power consumption by 48% and received power consumption by 27%.

INDEX TERMS 3GPP cellular networks (LTE/NR), handover, signaling overheads, power consumption, uplink reference signal, sounding reference signal (SRS), performance evaluation, simulation.

I. INTRODUCTION

The mobile communication industry has more than four billion users worldwide, that's more than half of the world's population [1]. The number of users is still growing exponentially. The data-oriented services including online gaming, high definition video streaming, and advancement in mobile application development prompt the cellular network operator to install additional base stations (BSs). Large scale small BS deployment can cause an escalation of the power consumption of the network that directly results in increased CO_2 emissions. More specifically, radio equipment at BSs is a major ''power consumer'' that accounts for around 70% of the total energy bill for the operators [2]. Thus, analyzing the power consumption at the BS is an effective approach that will provide a step forward to propose new schemes to reduce the power consumption at the Radio Access Network (RAN) and thus reduce the CO_2 emissions and increase the profitability of the operators.

According to the prior art, it is found that telecommunication is responsible for around 0.4 percent of CO_2 emissions worldwide [3]. The growing data rate demand of the user increases the associated power consumption that directly impacts the environment by contributing to global warming.

The associate editor coordinating the review of this manuscript and approving it for publication was Francisco Rafael Marques Lima.

Since operators' operational expenditures (OPEX), power consumption, and CO_2 emissions are inter-related, analyzing the power consumption during a HO scenario is a step forward to propose a power-efficient HO scheme. Increasing the system capacity by reducing the coverage of the BSs in current cellular networks (e.g. LTE and NR) increases the number of HOs, especially for high-speed users, who experience an increase in the signaling traffic. Here, and in the remainder of this paper, a BS could refer to either an LTE Evolved Node B (eNB) or an NR next-generation Node B (gNB). The failure of the signaling messages' transmission/reception introduces an increased system latency as well as an outage that might cause a loss of revenue for the operators. Therefore, one of the main issues is to identify the type and the number of signaling messages during HO which consumes the most energy. In this paper, we examine the different signaling message types produced during the HO procedure over the air-interface and study the impact of user speed, cell densification and HO parameter selection. Based on the signaling messages' transmission and reception, we compute the average transmitted (and received) power consumption values by using well-established power consumption models for both the BS and the UE. This helps to identify which part of the HO procedure is the main contributor to the overall power consumption.

A. UPLINK REFERENCE SIGNAL BASED MOBILITY

Current handover schemes rely on the measurement and subsequent measurement reporting done by UEs over downlink (DL) RS transmitted by nearby BSs. Notably, in dense cellular networks where serving BSs rapidly vary, it is important to reduce the energy consumption of the terminal by minimizing the measurement of such DL reference signals (RSs). Furthermore, reducing the measurement report transmission and other HO related signaling messages has also the potential for improving the UE battery lifetime. To this end, it is proposed [5], [24]–[26] that the UEs transmit UL RSs which are later to be measured by the network instead of relying on the UE measuring and reporting DL RS, as in traditional cellular mobility [5]. This way, the network can track and locate the mobile user using UL RS based measurements [5]. These measurements are processed in a central network controller that decides which BS will serve the user. Using this method, periodic measurement reports between UE and network are not required, thus reducing the HO related signaling messages as well as power consumption.

The Sounding Reference Signal (SRS) is a reference signal transmitted by the UE in the uplink (UL) direction that is used by the BS to estimate the quality of the UL channel in both LTE and NR standards [38], [39]. The SRS is typically estimated for large bandwidths outside the span scheduled to a UE [4]. The SRS-based channel estimate is used for efficient scheduling i.e. assisting the UL medium access control (MAC) scheduler in allocating UEs to resource blocks (RBs). The BS can also use SRS to estimate UL timing for timing alignment procedure. More recently, NR also uses the SRS for link adaptation, efficient scheduling, massive MIMO, and beam management. Similarly, there is another UL RS in LTE/NR, the DMRS (Demodulation RS), which provides channel information on the scheduled band for a particular UE. In the following, we will simply refer to UL RS noting that, implementation-wise, we could use either the SRS or the DMRS to realize the UL RS based mobility.

B. RELATED WORK

Many BS power consumption models are available in current literature, whereas handset power consumption models are less so. In [6], [7], the main power-consuming elements were considered to calculate a simplified BS power consumption model. An LTE smartphone overall power consumption model was proposed in [8]. The energy consumption of different radio access technologies (RATs) was compared using an energy consumption gain metric in [9] revealing that the LTE RAT is the most energy-efficient when compared to GSM and UMTS. Data rate and power consumption tradeoff have been discussed e.g. in [10], [11]. Energy consumption analysis of device to device (D2D) communication in 5G systems was presented in [11] that used 3GPP LTE and WiFi models to analyze the power consumption of both the BS and the UE. It was found that the best option to save energy is to minimize the number of active interfaces and send the data with the maximum possible data rate. Studying the effect of mobility in energy consumption was proposed as a future interesting topic. A solution to the power allocation problem in a neighborhood area network (NAN) with femtocell and relay technology is investigated in [12]. The results show that the average transmit power required for transmission through femtocell is 99% less in comparison to cooperative transmission (smart meter communicating with relay nodes). A two time-scale cross-layer resource allocation algorithm is proposed in [13] to guarantee reliable data transmission while minimizing the energy cost.

In related works, a HO strategy to minimize the energy consumption at BS in HetNets was proposed in [2] that only considers the energy consumption during the HO execution phase. This technique reduces the number of unnecessary HOs, thus improving energy consumption. A distributed mobility robustness optimization algorithm is proposed in [14] to minimize HO failures due to radio link failure (RLF) by adjusting HO related parameters (i.e. time to trigger and offset parameters). The algorithm classifies too early, too late, and wrong cell HO failure categories and optimizes the HO parameters according to the dominant failure. An early HO procedure is proposed in [15] to reduce the RLF, ping pong events and energy consumption, at the cost of keeping the other performance parameters within acceptable limits. A HO skipping technique for 4G and 5G systems is proposed in [16] to reduce the HO rate. Similarly, a location-aware, cell size aware and hybrid HO skipping technique to reduce the HO rate is also proposed in [17]. However, at high speeds, estimating the serving area of the cell and user trajectory to make a HO skipping decision is challenging. A HO technique for

ultra-reliable low latency communication is proposed in [18] to improve the HO delays and energy efficiency. The role of the source gNB in deciding the target cell is bypassed and a direct HO request from the UE to the target gNB is proposed. In the case where the HO request is rejected by the target cell, the proposed system fallbacks to the existing gNB assisted HO which further increases the HO delay. In our previous work [19], we found that increasing/decreasing the inter-site distance (ISD), after a certain limit, degrades the HO performance mainly due to limitations in the UL. In [20], we included a power consumption model for the transmitted signaling messages during handover. We showed that, although the measurement report (MeasReport) transmission is the major contributor to the air-interface signaling, random access channel (RACH) transmission is the main power consuming contributor due to its higher utilization of the resources (i.e. resource blocks). We also proposed a receiver power consumption model in [21].

The work in [5] proposes a user-transparent mobility concept based on the transmission of UL RS (beacons) using Zadoff-Chu signature sequences for reliable detection at the BS. The suitability of beacon resources, as well as the reliability of the proposed beacon design, was validated to highlight its advantages over legacy HO mechanisms. The idea of joint tracking of a group of users with UL RS has also been proposed in [22]. An accurate device positioning and tracking algorithm for the 5G ultra-dense network has been proposed in [23] by utilizing the UL RS. An extended Kalman filter (EKF) based solution is formulated for efficient joint estimation and tracking of the direction of arrival (DoA) and time of arrival (ToA) of the user nodes (UNs) using UL RS. In order to fuse the individual DoA and ToA estimates across one or more access nodes (ANs) into an accurate UN position estimate, a second EKF stage is added which also provides accurate clock offset estimates and reliable clock synchronization of the access link.

An UL RS based mobility management scheme is proposed in [24] for the 5G system. The simulation results show that this technique can save UE power consumption by up to 63% in comparison to the traditional DL mobility method. Similarly, a UE power consumption comparison between UL and DL-based mobility is presented in [25]. The analysis shows that the UL mobility scheme outperforms over DL mobility for ''Rural with high-speed UEs'' and high gain in terms of UE power consumption is observed especially for the ''high-speed train'' scenario. The work in [26] suggests that UL mobility can reduce the HO failure rate and the UE power consumption in NR. In [24]–[26], the authors seem to address the UE power consumption only, whereas we provide both UE and BS power consumption analysis.

This work is the extension of our previous works [20], [21] with added novelty which comes from the overall power consumption model (for both transmission and reception of the signaling messages over the air-interface), the calculation of the transport blocks (TBs) used for each signaling message according to the 3GPP specified standards and UL RS based power efficient HO procedure. To the best of our knowledge, the study of air-interface signaling, the overall power consumption of the HO procedure, and the concept of using UL RS to make the HO procedure power-efficient have not been addressed in the literature.

C. MAIN OBJECTIVES AND CONTRIBUTIONS

The main objectives of this work are to investigate the power consumption associated with HO signaling in 3rd Generation Partnership Project (3GPP) cellular networks (i.e. LTE/NR) and to define a power-efficient HO scheme based on UL RSs for future 3GPP standards. The utilization of UL RSs in the HO procedure is mainly motivated by the evolution of mobile network generations towards ultra-dense networks operating at higher–frequencies and implementing a user-centric no-cell approach (UCNC) [27]. UCNC aims at supporting massive connectivity while turning all users to cell-center users. UCNC is expected to be fully implemented in B5G mobile networks, however, it can be to some certain extend implemented in any radio access technology that supports SRS incl. 4G, 5G, and 6G. To this end, our proposed UL RS-based HO scheme is RAT-agnostic and future proof as compared to the legacy HO procedure which doesn't scale. In fact, the legacy HO procedure in both NR and LTE follows the same principles, with only minor nomenclature differences [28]. For the performance evaluation section, however, we will compare our UL RS-based HO approach with LTE which provides the most challenging and pronounced reference scenario that our HO procedure can further optimize. Furthermore, future open radio access network (O-RAN) standard specifications aim at specifying a RAN architecture that relies on a software-based radio resource management (RRM) platform of functions including energy-efficient HO as herewith proposed [29]. Such a software platform will allow both NR and LTE to follow their own evolution and optimization, given their actual deployment worldwide.

The first contribution of this study is to analyze the power consumption of the different signaling types during a HO procedure for different cell sizes. As a result, an optimum cell size with regards to power consumption is identified. For this purpose, a detailed model of transmitted and received power consumption for HO message signaling is developed. Based on the model, transmitted and received power consumption values during HO can be obtained. In alignment with our previous studies [20], [21], our analysis shows that the MeasReport transmission is the major contributor to the air-interface signaling.

The second contribution of this work is that it provides a solution to cope with the problem of high power consumption due to MeasReport signaling. We propose a power-efficient HO measurement procedure based on UL RSs, and we specifically use the Sounding Reference Signal (SRS) available in LTE/NR. We implement the UL RS based mobility in a system-level simulator to compare the performance of HO with traditional DL based measurement. In this work, we mainly compare the power consumption of DL and UL RS

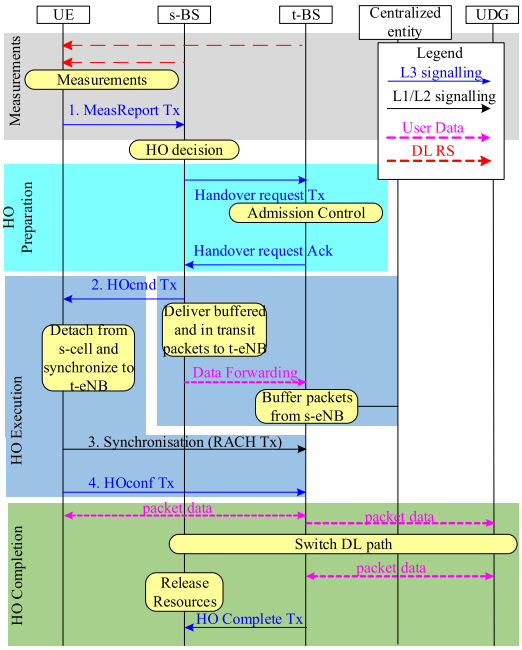

FIGURE 1. **Current cellular networks HO Procedure (adapted from [30], [31]).**

based mobility to quantify the potential benefits. Using this method, no measurement report is needed to be transmitted from the UE to the BS, thus it improves the UE battery lifetime, reduces the OPEX and environmental effects.

The remaining sections are organized as follows: Section II provides a summary of the HO mechanism in LTE/NR cellular networks. Section III discusses the simulator modeling aspects with transmitted/received power consumption models for both the UE and the BS. In Section IV, an analysis based on the simulation results is presented. Finally, Section V provides some concluding remarks.

II. OVERVIEW OF HANDOVER MECHANISM IN 3GPP CELLULAR NETWORKS

A brief summary of the HO procedure in 3GPP cellular networks is shown in Fig. 1 [30], [31]. As per the standardized technical specification, 3GPP TS 36.300 [30] and TS 38.300 [31], 3GPP is still relying on the DL measurement-based handover (HO) procedure for both LTE and NR (identical in both RATs except for some entity renaming). Hereafter, we will adopt a generic naming convention as a way to indistinctively refer to both LTE and NR use cases. For example, the user data gateway (UDG) in Fig. 1 is the serving gateway (SGW) in LTE and the User Plane Function (UPF) in NR. Similarly, the centralized entity in Fig. 1 is the Mobility Management Entity (MME) in LTE and the Access and Mobility Management Function (AMF) in NR. Finally, in our proposed HO scheme, we will use the term BS referring to either an LTE eNB or an NR gNB. The procedure is divided into 3 phases: HO preparation, HO execution, and HO completion phase. Upon measuring and identifying a better neighboring cell, the UE reports to the serving BS (s-BS) and accesses the target BS (t-BS) subsequent to the reception of a HO command (issued from the s-BS). The UE performs signal strength measurements over specific RS resources and computes the reference signal received power (RSRP) from the s-BS as well as the neighboring cells. After processing the measurements, including filtering at layers L1 and L3, if an entry condition is fulfilled, a measurement report (MeasReport) is transmitted to the s-BS. The A3 event is used as an entry condition described as the RSRP of the t-BS being higher than that of the s-BS plus a hysteresis margin (called A3 offset). This entry condition has to be maintained during a time defined by the time to trigger (TTT) timer [30]. Once the MeasReport is correctly received at the s-BS, the HO preparation phase between the s-BS and the t-BS starts with a HO request transmitted from the s-BS to the t-BS. Upon successful admission, the t-BS acknowledges the HO request sent by the s-BS and prepares for HO. Subsequently, a HO command (HOcmd) is transmitted from the s-BS to the UE. If successful, the HO execution phase starts in which the UE accesses the t-BS by means of synchronization and Random Access Channel (RACH) transmission, followed by the transmission of a HO confirmation (HOconf) message. Finally, the t-BS transmits a HO complete message to the s-BS to inform the success of the HO when the DL path is switched toward the t-BS. After that, the s-BS releases the allocated resources. In the described context, HO optimization deals with the adjustment of the TTT, the L3 filter coefficient (K), and the A3 offset to achieve a good compromise between HO frequency and HO reliability [32].

A. UPLINK REFERENCE SIGNALS BASED MEASUREMENT PROCEDURE

Whereas the current HO measurement procedure in LTE/NR is based on UE measurements over DL RSs, in this paper we propose the HO measurements to be performed at the BSs, over UL RSs transmitted by the UEs. To this end, we note that current standards include UL RS transmission and measurements for various purposes (e.g. link adaptation, channel estimation, beam management, etc.). In this paper, we further extend the applicability of UL RS for handover. In particular, the sounding reference signal (SRS), defined in both LTE and NR (see [38], [39]), will be used as described hereafter.

As illustrated in Fig. 2, the UE transmits UL RSs which are received at the serving and, possibly, several neighboring BSs (n-BSs), allowing the network to perform UL signal strength measurements. These measurements are processed in a central network controller to make intelligent proactive decisions on which BS shall serve a given user. The realization of the UL-HO scheme comes with the requirement that the time synchronization between the BSs receiving the UL RS should be within some specified upper bound. This requirement may already be in place to efficiently support other implementations such as TDD operation, joint uplink transmission, etc. in small cell deployments with very short propagation times. In addition, in order for a n-BSs to be able to detect and measure the UL RS, it is also required that the

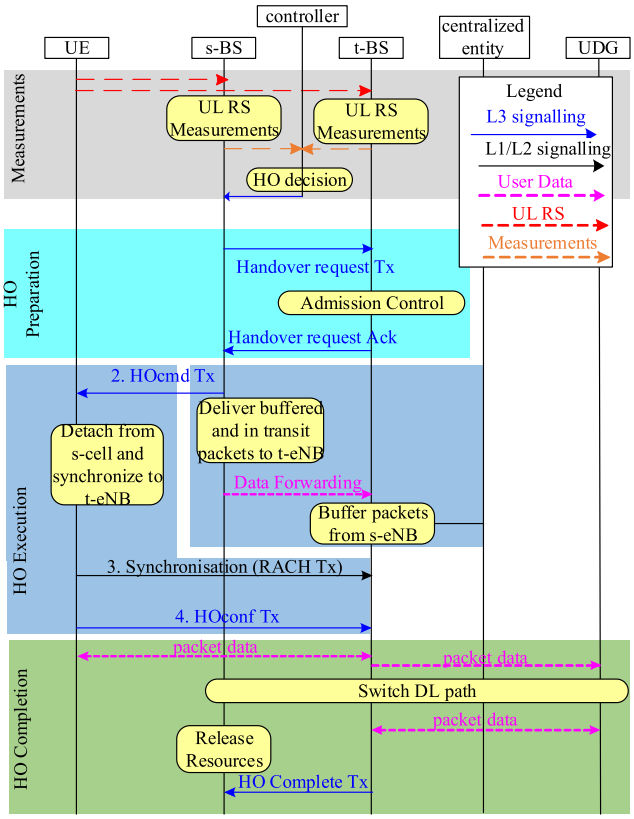

FIGURE 2. Uplink Reference Signal based HO Procedure (adapted from [5], [30], [31]).

configuration parameters (timing, frequency, code, etc.) of such UL RS, which are set by the s-BS, are also shared with n-BS. This can be effectively achieved via existing interfaces (such as e.g. X2 or S1 in LTE) and would only require some minor standard upgrades in defining the information elements to be communicated between the BSs. From a power control perspective, note that there is only a need for n-BSs to detect and measure the UL RS when the UE is approaching the cell border, i.e. where handovers take place. When this happens, the power control set by the s-BS should allow the UL RS to be received at the n-BS, since both the s-BS and n-BS become almost equidistant (in radio terms that is). Furthermore, the detection of UL RS is rather robust since it is, by design, a known signal transmission, with known time, frequency and code signatures and thus easily detectable and measurable at the n-BSs.

The rest of the HO procedure remains the same as in LTE and NR starting from the HO preparation phase in Fig 1. By reusing the UL channel measurements from UL RSs (needed in, e.g., massive MIMO operation) also for mobility purposes requires no extra signaling overhead. Another benefit of using UL measurements for UE mobility is that it is possible to improve the network performance by network-side upgrades without UE impact. The network controller measurement processing procedure is shown in Fig. 3. As the UE moves through the network, the serving BS becomes weaker than the target BS. The serving, as well as n-BSs,

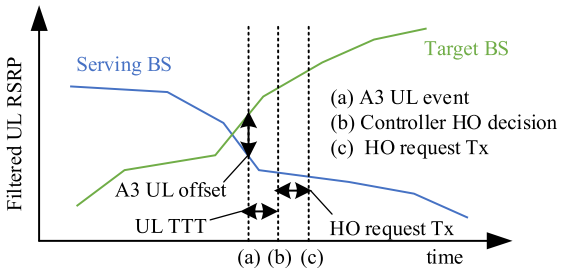

FIGURE 3. Network controller measurement processing.

perform UL RS received power (UL-RSRP) measurements and these measurements are processed in a central network controller. If the UL-RSRP of the serving BS is less than a target BS by an offset called "A3 UL-offset", and this condition is maintained during the time defined by "UL Time To Trigger (UL-TTT)", the controller decides which BS shall serve the given UE. Based on the controller HO decision, the serving BS sends a HO request to the controller suggested target BS.

III. SYSTEM MODEL

A hexagonal grid of 16 tri-sectored BSs is considered in a MATLAB based system-level simulator. In order to ensure fair interference conditions across the simulation scenario, cell wrap-around feature is included. A total number of 100 UEs (with fixed speed and random directions [0°, 360°]) are placed randomly over the simulation scenario.

For traffic loading, UEs with UL full-buffer traffic are considered, thus contributing to UL interference towards other UEs. DL interference is artificially generated by setting the transmission power on a number of randomly selected Physical Resource Blocks (PRBs) given a specific load level (in our case a fully loaded case is assumed).

Some of the main features of physical (PHY), Medium Access Control (MAC), Radio Link Control (RLC) and Packet Data Convergence Protocol (PDCP) layers are implemented in the simulator including, segmentation, inter alia, MAC scheduling with chase combined Hybrid-ARQ (HARQ) and Automatic Repeat Request (ARQ) at RLC level. Look-up tables are used for the PHY layer to map bit error rate (BER) values to subcarrier measured signal-to-interference-plus-noise ratio (SINR) values (via the effective exponential SNR mapping (EESM)) to account errors in the wireless link.

The modeling of Layer-3 (L3) RRC signaling (including measurement report, HO command, and HO confirmation) over the radio access is considered in the HO model. PDCCH is modeled to capture Layer-2 (L2) signaling (DL and UL allocation). These signaling messages are subject to channel impairments and thus suffer from RLC failures. Moreover, the simulator also considers Radio Link Failures (RLFs) which are triggered under different circumstances related to the unacceptable quality of the radio link [35]. The simulation implementation is largely based on LTE. Given the similar nature of LTE and NR HO procedures, the expected

TABLE 1. Simulation parameters and assumptions.

Feature	Implementation
Network topology	A hexagonal grid of 16x3=48 cells (wrap-around included)
Inter-site distance	From the set {125, 250, 500, 750, 1000, 1250} m
System Bandwidth	B_{sys} =5 MHz (paired FDD), with $N_{RB}^{DL} = N_{RB}^{UL} =$ 25 RBs at carrier frequency f_c =2.1GHz, 1TB=6 RBs, $N_{TB}^{DL} = N_{TB}^{UL} = \lfloor 25/6 \rfloor$
BS DL power	$P_{eNB} = 43$ dBm
UE Power	$P_{UE} = 23$ dBm
Antenna patterns	3D model specified in [34], Table A.2.1.1.2-2
Channel model	6 tap model, Typical Urban (TU)
Shadowing	Log-normal Shadowing Mean 0 dB, Standard deviation: 8dB
Propagation model	$L = 130.5 + 37.6 \log_{10}(R)$, R in km
UE speed	{3, 30, 60, 120} km/h
RLF detection by L1 of UE	T310=1s, N310=1, N311=1 as specified in [35] Q_{in}=-4.8 dB; Q_{out}=-7.2 dB as specified in [36]
HO parameters	TTT= {32} ms, A3 offset = {1} dB, L3 filter coefficient K=4 (fixed).

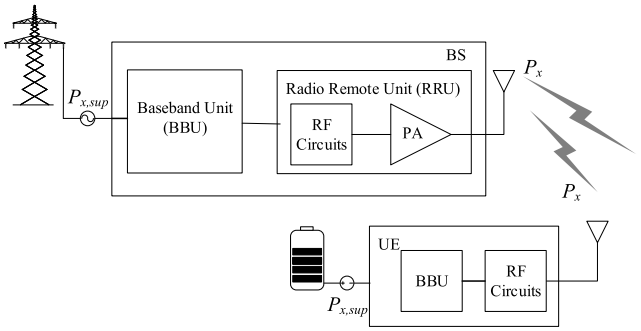

FIGURE 4. A simplified overview of the BS and UE components included in the transmitted power model.

evaluation in an NR simulator would comparatively provide similar outcomes. Table 1 summarizes the main simulation assumptions.

A. TRANSMITTED POWER CONSUMPTION MODEL

In the BS, the radio equipment can be largely divided into the Base-Band Unit (BBU) and the Remote Radio Unit (RRU). A BBU is responsible for communication through the physical interface. The BBU is placed in the equipment room and connected with RRU through an optical fiber. An RRU is configured to communicate with the UE through the air interface. The units comprising the RRU (the RF circuit and power amplifier unit) perform inter-conversion between the digital signal and RF signal, associated preprocessing, amplification, and filtering, etc. A simplified overview of the BS and UE components included in the transmitted power consumption model is shown in Fig. 4, where $P_{x,sup}$ denotes the necessary supply power to produce an output (transmitted) power P_x, see e.g. [37], where $x = \{BS, UE\}$. We are interested in the contribution of the HO mechanism towards supply power $P_{x,sup}$.

Specifically, we focus on the HO signaling over the air interface in both UE (UL) and BS (DL) transmissions,

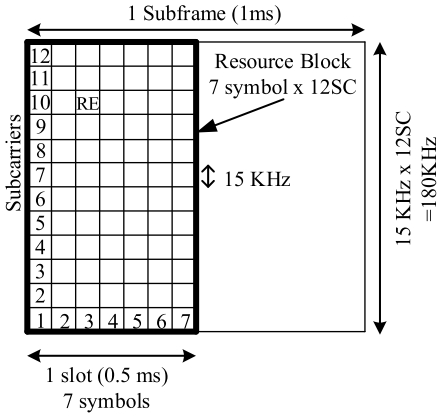

FIGURE 5. A resource block illustration [42].

namely: the HOcmd transmission from the BS side, labeled as (2) in Fig. 1, and the MeasReport, the RACH and the HOconf transmission from the UE side, labeled as (1), (3) and (4) respectively. To derive the power consumption of the above-mentioned signaling messages transmissions, we first find the size of such messages, then the amount of frequency resources (PRBs) needed to transmit these messages, and next the output transmitted power allocated to these resources. Finally, a time duration of these messages or duty cycle is used to compute the time-averaged supply power consumption.

In LTE, the smallest time-frequency unit allocated to a user is a resource block (RB), illustrated in Fig. 5. For a subcarrier spacing of $\Delta f = 15$ kHz, a RB has a bandwidth of $B_{RB} =$ 180 KHz (i.e. $N_{sc}^{RB} = 12$ subcarriers) and a time duration of one slot, $T_{RB} = T_{slot} = 0.5$ ms [38]. Alternatively, the RB (or slot) duration can be expressed in terms of the number of symbols; it contains, $N_{symb}^{RB} = 7$, times the symbol length T_{symb}. The smallest resource unit consisting of one symbol and one subcarrier to which a modulated symbol is mapped onto is defined as a resource element (RE). According to the available modulation schemes in LTE, the number of carried bits in a single RE is $L_{RE} \in \{2, 4, 6\}$ bits for QPSK, 16-QAM, and 64-QAM modulation respectively. A transport block (TB) is the amount of data that the upper layer (MAC layer) provides to the PHY layer depending on modulation and coding scheme (MCS) and cyclic redundancy check (CRC).

It is worthwhile noting that because HOs occur mostly at the cell edge, where the RSRP is low, this justifies our selection of QPSK as the modulation scheme used for the transmission of signaling messages (see Table 2 for details). To transmit MeasReport data bits in one TB, we assume 1 ms subframe with 6 RBs and 2 slots. We also assume the modulation and coding scheme (MCS) index $I_{MCS} = 0$ (very low) as a bottleneck slowing down the flow of HO messages. The size of each signaling message (in bits) is denoted by L_s, with subindex $s = \{MR, HOcmd, HOcnf\}$. Now we can find the number of information bits per TB ($L_{TB} = 152$ *bits*) using [40] that include 128 bits of the MeasReport Tx and 24 CRC bits.

TABLE 2. Power consumption parameters and values.

Feature	Values
Signaling message sizes	$L_{MR} = 128$ bits; $L_{HOcmd} = 296$ bits; $L_{HOcnf} = 96$ bits (according to [41])
Carried bits in a TB	L_{TB} =152 bits (with QPSK modulation, $L_{RE} = 2$, MCS index=0) [40]
Number of TBs per each signaling message	$N_{TB}^{MR} = 1$ TB; $N_{TB}^{HOcnf} = 1$ TB; $N_{TB}^{HOcmd} = 2$ TBs; N_{TB}^{RA} =1 TB.
Power Amplifier efficiency	$\eta = 0.311$ (31.1%) [6]
RF supply power	$P_{RF,BS} = 12.9$ W [6] and $P_{RF,UE} = 2.35$ W [8] scaled according to used bandwidth
BBU power	$P'_{BB} = 29.4\,W$ [7], $P_{TxBB} = 0.62\,mW$ [8], $P_{RxBB} = 0.97.R_{Rx} + 8.16$ (mW) [8]
Signaling transmission times	$T_{BS}^{HOcmd} = 1$ms; $T_{UE}^{MR} = 1$ms; $T_{UE}^{HOcnf} = 1$ms; $T_{UE}^{RACHtx} = 1$ ms (we use preamble format 0 according to the cell radius used in simulations, as noted in [42]);

With the above in mind the required number of TBs for each signaling message s, N_{TB}^{s}, can be obtained by:

$$N_{TB}^{s} = \left\lceil \frac{L_s}{L_{TB}} \right\rceil, \quad \text{with } s = \{MR, HOcmd, HOcnf\}, \quad (1)$$

where $\lceil x \rceil$ denotes the smallest integer larger than or equal to x, and, hence it is assumed herein that a signaling message requires an integer number of TBs. In addition, for the RACH signaling message transmission, since it carries an un- modulated preamble sequence, we can directly refer to the standard specifications which provide us with the value of N_{TB}^{RA} [38] (see Table 2). The power allocation algorithm in both the BS and the UE will adjust the power level assigned to each subcarrier (and therefore RB and TB) according to the maximum available powers in the BS (P_{BS}) and in the UE (P_{UE}) (see Table 1). For the case of an equal power allocation algorithm, the allocated power per TB at the BS and UE can be formulated as:

$$P_{BS}^{TB} = P_{BS} \Big/ N_{TB}^{DL}, \quad \text{and} \quad (2)$$

$$P_{UE}^{TB} = P_{UE} \Big/ N_{TB}^{UL}, \quad (3)$$

where N_{TB}^{DL} (N_{TB}^{UL}) is the total number of TBs in the DL (UL) given a system bandwidth B_{sys} (see Table 1).

The allocated transmitted power (in W) per signaling message s is:

$$P_{x,Tx}^{s} = P_{x}^{TB} \cdot N_{TB}^{s}, \quad (4)$$

where $x = \{BS, UE\}$ and, accordingly, the appropriate number of DL or UL signaling messages should be reflected in N_{TB}^{s}.

We now may apply some well-known power consumption models for both the BS and UE, [6], [8], in order to obtain the supply power necessary to produce the required transmitted power for each of the signaling messages. In particular, the supply power for the BS transmitting signaling s, $P_{eNB,sup}^{s,Tx}$, can be written as

$$P_{BS,sup}^{s,Tx} = P_{BS,Tx}^{s} \Big/ \eta + N_{TB}^{s} \Big/ N_{TB}^{DL} .(P_{RF,BS} + P'_{BB}), \quad (5)$$

where $P_{BS,Tx}^{s}$ is the output transmitted power given by (4) and η is the power amplifier efficiency. $P_{RF,BS}$ denotes the supply power contribution of the RF equipment, which is conveniently scaled by the portion of utilized resources by signaling message s. Similarly, P'_{BB} is the basic BBU consumption in watts (see Table 2) [7].

Equally, the supply power required for the UE to transmit signaling message s, $P_{UE,sup}^{s,Tx}$, is given by

$$P_{UE,sup}^{s,Tx} = P_{UE,Tx}^{s} + N_{TB}^{s} \Big/ N_{TB}^{UL} .(P_{RF,UE} + P_{TxBB}), \quad (6)$$

where, $P_{UE,Tx}^{s}$ is the output transmitted power given by (4), and where the supply power contribution to the RF and BB part is also scaled by the portion of utilized resources by signaling s. P_{TxBB} is the transmitted UE BBU power (see Table 2) [8].

We define the time-averaged supply power in (7) to capture the time-domain system dynamics during transmission and possible retransmissions of signaling messages,

$$\bar{P}_{x,sup}^{s,Tx} = P_{x,sup}^{s,Tx} \cdot (\Delta t_x^s / \Delta T), \quad (7)$$

where $P_{x,sup}^{s,Tx}$ ($x = \{BS, UE\}$) is the "peak" supply power defined in (5)-(6), and $(\Delta t_x^s / \Delta T)$ represents the duty cycle or percentage of time where the signaling is actually transmitted. Assuming that the signaling s has a duration of T_x^s seconds (refer to Table 2 for details) and that a number of N_s signaling messages are transmitted over a period of ΔT seconds, we get $\Delta t_x^s = T_x^s \cdot N_s$. Finally, we are able to rewrite (7) as:

$$\bar{P}_{x,sup}^{s,Tx} = P_{x,sup}^{s,Tx} \cdot T_x^s \cdot \left(N_s / \Delta T\right) = P_{x,sup}^{s,Tx} \cdot T_x^s \cdot R_x^s, \quad (8)$$

where we have defined $R_x^s \left(N_s / \Delta T\right)$ as the signaling rate which will be obtained from system-level simulations. The main numerical parameters used in the simulations are shown in Table 2.

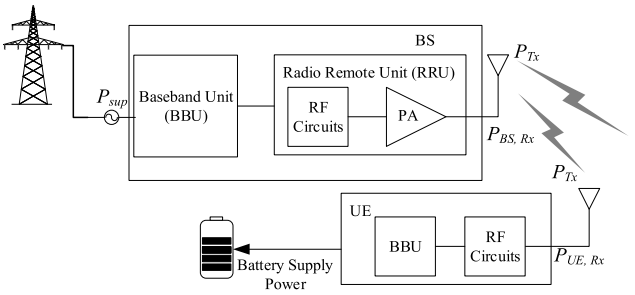

FIGURE 6. A simplified overview of the BS and UE components included in the received power model.

B. RECEIVED POWER CONSUMPTION MODEL

A simplified overview of the BS and UE components included in the received power model is shown in Fig. 6, where P_{Rx} is the received power. We are interested in the

contribution of the HO mechanism towards supply power $P_{x,sup}$ necessary to retrieve the data.

The received power (in W) per signaling message s is obtained using the system level simulator that follows the below expression,

$$P^{s}_{x,Rx} = P^{s}_{x,Tx}.G_{i,j}.|h|^2 + P^{s}_{n}, \quad (9)$$

where $x = \{BS, UE\}$ and, $G_{i,j}$ is the total path gain for i^{th} UE and j^{th} t-BS (including distance-dependent attenuation, the angular antenna gain, and shadow fading), $|h|^2$ is the fast fading contribution and, finally, P^{s}_{n} is the additive white Gaussian noise contribution over the bandwidth of signaling message s.

We now may apply some well-known power consumption models for both the BS and UE, [6], [8], in order to obtain the received power necessary to receive the data for each of the signaling messages. In particular, the supply power for the BS signaling s reception, $P^{s,Rx}_{BS,sup}$, can be written as

$$P^{s,Rx}_{BS,sup} = P^{s}_{BS,Rx}/\eta + N^{s}_{TB}/N^{DL}_{TB}.(P_{RF,BS} + P'_{BB}), \quad (10)$$

where $P^{s}_{BS,Rx}$ is the received power given by (9) and η accounts for the power amplifier efficiency. Equally, the supply power for the UE to receive signaling message s, $P^{S,Rx}_{UE,sup}$, is given by

$$P^{s,Rx}_{UE,sup} = P^{s}_{UE,Rx} + N^{s}_{TB}/N^{UL}_{TB}.(P_{RF,UE} + P_{RxBB}(R_{Rx})), \quad (11)$$

where, $P^{S}_{UE,Rx}$ is the received power given by (9), and where the received power contribution to the RF part is also scaled by the portion of utilized resources by signaling s. P_{RxBB} is the received BBU power (see Table 2) where R_{Rx} is the received data rate that can be found as $R^{s}_{x} \cdot L_{TB}$ [8].

Now, the time-averaged supply power can be written as,

$$\bar{P}^{s,Rx}_{x,sup} = P^{s,Rx}_{x,sup} \cdot T^{s}_{x} \cdot (N_s/\Delta T) = P^{s,Rx}_{x,sup} \cdot T^{s}_{x} \cdot R^{s}_{x}, \quad (12)$$

C. UPLINK REFERENCE SIGNALS MODEL

The SRS based module has been modeled as per 3GPP standards described in [38], [40] and integrated with the system-level simulator. The resources assigned for SRS can be distributed in the time, frequency, and sequence plane as shown in Fig. 7. A part of the system bandwidth is used for SRS, at each SRS transmission occasion which occurs at a given SRS periodicity. Each Zadoff-Chu sequence is transmitted in a limited bandwidth (B_{SEQ}), which determines the number (N_{SrsRB}) of SRS RBs that can be transmitted in each SRS transmission occasion. A number of orthogonal sequences (M_{SEQ}) can be sent in parallel in the same resource block. These sequences are generated from ($|q|$) different root sequences and (α_{SEQ}) cyclic shifts of each root sequence. It is assumed that BSs coordinate with each other when allocating their SRS resources to their associated UEs to avoid pilot contamination. By selecting these parameters appropriately the resources for SRS can be dimensioned. The SRS parameters

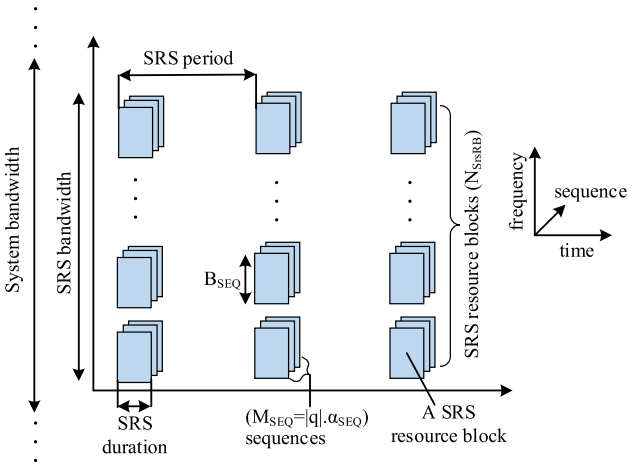

FIGURE 7. SRS resource dimensioning [5].

TABLE 3. SRS parameters and values.

Feature	Values
SRS periodicity	{5ms, 10ms, 20ms, 40ms, 80ms, 160ms, 320ms} [40] Table 8.2-1.
Number of transmission combs (K_{TC})	2 [38]
Number of SRS antenna ports	1 (used for sounding)
Number of OFDM symbols for an SRS resource	1
SRS number of symbol per slot	1
Cyclic shift	{0, 1, 2,……,7} for K_{TC}=2 [38]
Bandwidth Configuration (C_{SRS})	7, choices {0, 1, 2, ……,7}[38]
Bandwidth (B_{SRS}) in PRBs	12
SRS frequency hopping bandwidth	0, choices {0, 1, 2, 3} [38]
SRS configuration index (I_{SRS})	Range=0 to 636, [40]
SRS duration	0.5ms (1 slot)
Root sequence |q|	(u,v) where u= sequence group number= {0,1,...29} and v= base sequence number within the sequence group = {0,1} [38]

used in the system-level simulator are explained in Table 3. The SRS parameters terms are explained as following [40],

SRS Periodicity: it is the tendency of SRS transmission/reception to recur at specified intervals. The SRS periodicity ranges from 2ms to 320ms. This is calculated by the SRS Configuration Index (I_{SRS}). In this work, we consider different SRS periodicities to see the impact on power consumption and to find an optimum SRS periodicity value.

SRS Power: we assume that the SRS subcarriers and non-SRS subcarriers are allocated with the same power.

Transmission Comb (K_{TC}): the transmission Comb values are 0 or 1 that informs whether to transmit SRS in every odd or even subcarrier within the SRS bandwidth. Using K_{TC} values (0 or 1), the BS can multiplex two UEs with the same frequency, cyclic shift, and time resources.

Cyclic Shift: it can vary from one to eight for $K_{TC} = 2$ which generates up to eight different orthogonal SRSs. Using

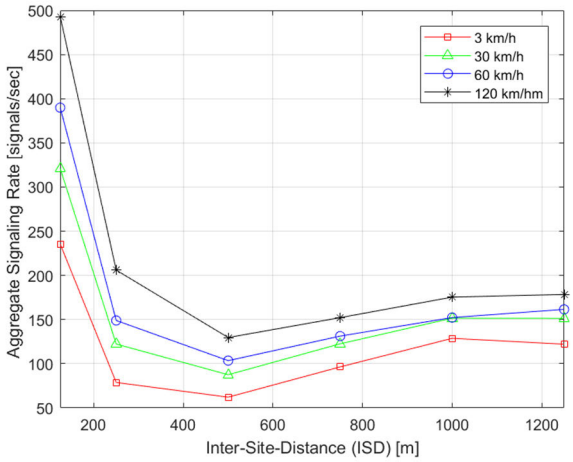

FIGURE 8. Impact of ISD and UE speed on the aggregate signaling rate.

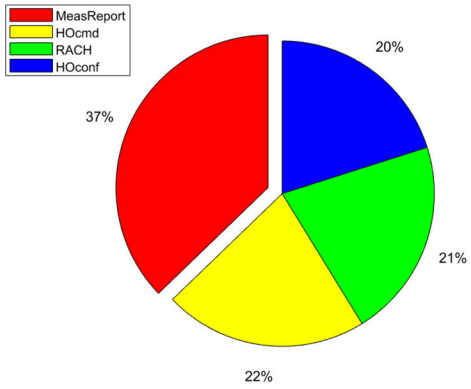

FIGURE 9. Average distribution of signaling rate per type.

cyclic shift, the BS can configure SRS for up to eight UEs in the same frequency resources and subframe using different cyclic shift values {0, 1, ...,7}.

SRS Frequency Hopping Bandwidth: this is defined for the frequency hopping purpose of SRS. If the frequency hopping is enabled, then SRS frequency hopping bandwidth will be smaller than SRS bandwidth (B_{SRS}).

IV. SIMULATION RESULTS

A detailed numerical evaluation is provided in this section for the HO procedure in terms of both signaling and power consumption costs. Also, a detailed comparison of the power consumption of DL and UL RS based method is provided.

A. DOWNLINK BASED HANDOVER RESULTS

This section provides the simulation results for the signaling rate and average supply power for both transmission and reception of the HO related signaling messages during the DL based HO procedure.

1) HANDOVER SIGNALING RATE ANALYSIS

This subsection provides the simulation results for the signaling rate during the HO procedure. The considered signaling messages transmitted over the air interface are: MeasReport, HOcmd, RACH and HOconf. Simulations are performed according to the models presented in Sec. III and the results are analyzed for different cell sizes, UE speeds, TTT and A3 offset values at a fixed L3 filter coefficient K mentioned in Table 1.

Fig. 8 shows the impact of ISD and UE speed on an aggregate signaling rate (i.e. the sum of all considered signaling rate transmissions). One trend of the graph shows that increasing UE speed, increases the signaling rate especially at low ISDs (i.e. 125m). We can argue that for small ISDs, higher UE speeds will cause moving away from the source cell which may result in increased HO failure rate that further leads to an increased signaling rate Also, for low ISDs, an increased number of cell border crossing and high interference areas from the neighboring UEs result in increased HO rate and HO failure rate, thus experience a high signaling rate owing to successive signaling retransmissions.

The average distribution (in %) of the different analyzed signaling message types for all simulated cases of various ISD, UE speed, TTT and offset values is shown in Fig. 9. It is clear from the graph that the signaling rate distribution is dominated by the MeasReport transmission (37%). This is because the UL transmission suffers from different channel impairments, due to transmission range and interference, for particular cell sizes. As a consequence, MeasReport retransmissions are often triggered which produces performance degradation in terms of increased signaling rate.

In our previous studies [20], [21], we found that increasing the TTT and offset values reduces the aggregate signaling rate significantly but at the cost of increased HO failures [32]. On the contrary, low TTT and offset values have less HO failure cases, as early HO trigger prevents changing the radio link conditions [32].

2) TRANSMITTED POWER CONSUMPTION ANALYSIS

The simulation results of the average supply power consumption due to the various HO signaling messages transmissions are provided in this subsection.

a: UE TRANSMITTED POWER CONSUMPTION

The impact of ISD and UE speed on the average supply power consumption of the UE is shown in Fig. 10, as given by (8), at a constant TTT and offset values. More interestingly, it is clear from the graph that the lowest ISD has the highest power consumption then it decreases and after that, it starts increasing again for high ISDs because of the UL impairments as also noted in Fig. 8 and Fig. 9. The lowest power consumption is attained for ISD 500m, which constitutes an ''optimum'' ISD under the simulated assumptions. An ISD of 500m turns to be optimal since we are able to avoid the UL impairment problems arising for small ISDs (due to high interference from neighboring UEs) and large ISDs (due to low UE transmitted power at the cell edge), see also [19]. The other trend of the graph shows that increasing UE speed, increases power consumption, especially at low ISDs, due

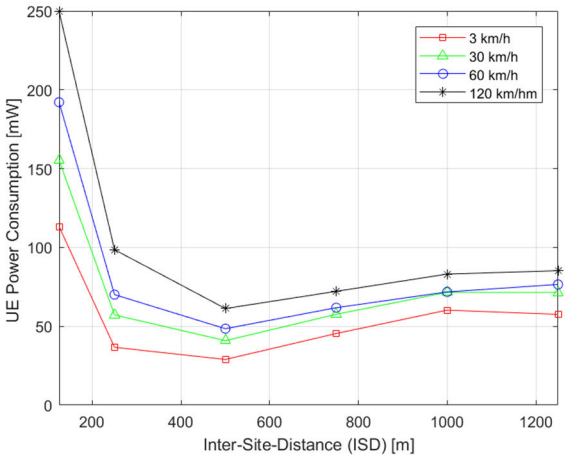

FIGURE 10. Impact of ISD and UE speed on the average supply power consumption of the UE, for offset = 1 dB and TTT = 32ms.

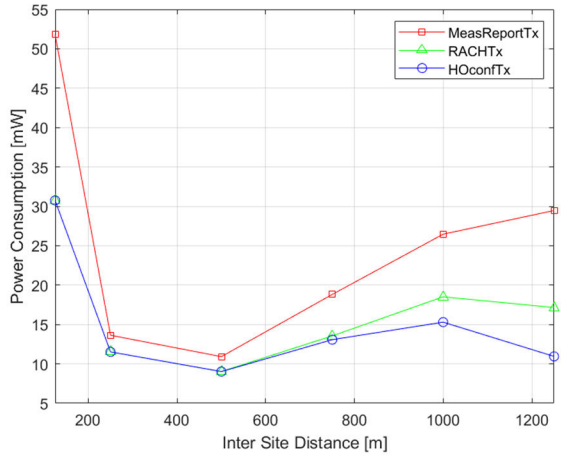

FIGURE 11. Impact of ISD on the average supply power consumption of various UE signaling messages transmission for speed = 3km/h, offset = 1 dB and TTT = 32ms.

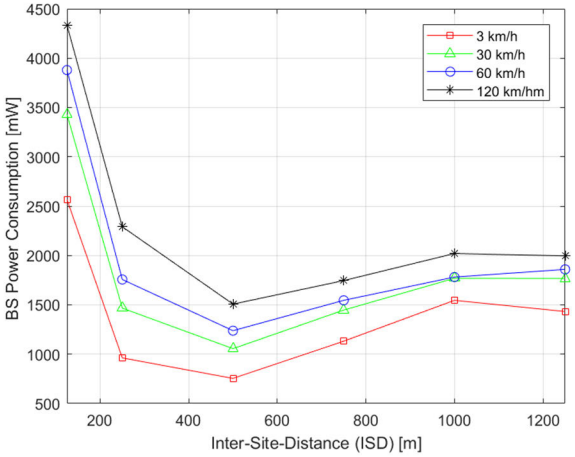

FIGURE 12. Impact of ISD and UE speed on the average supply power consumption of the BS, for offset = 1 dB and TTT = 32ms.

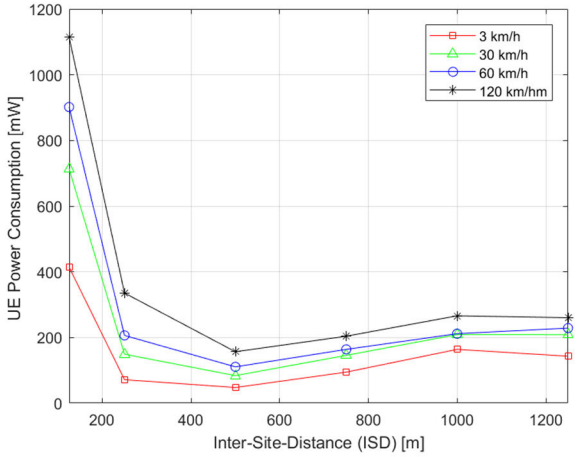

FIGURE 13. Impact of ISD and UE speed on the average supply power consumption of the UE received signaling messages, for offset = 1 dB and TTT = 32ms.

to the high signaling rate observed in Fig. 8. The steepest increase in the UE transmitted power consumption is found as we move from an ISD of 250m to an ISD of 125m ranging between 150% and 175% with decreasing mobility. Similarly, increasing offset and TTT values, the same trend is observed as noted in Fig. 8 and Fig. 9.

A per-type signaling power consumption breakdown for the UE is shown in Fig. 11. The largest contributor to power consumption is the MeasReport transmission by the UE because of the same reasons as noted in Fig. 9. The higher power consumption due to MeasReport Tx is being especially detrimental to battery-powered devices. Similar to the signaling rate case, increasing the TTT and the offset enforce a reduction of the signaling which significantly reduces the power consumption. However, this signaling and power reduction comes at the cost of increased HOFs as noted in [19].

b: BS TRANSMITTED POWER CONSUMPTION

The impact of ISD and UE speed on the average supply power consumption of the BS is shown in Fig. 12, as given by (8), at a constant TTT and offset values. The power consumption of HOcmd Tx (BS/DL power consumption) is much higher as compared to others (UE/UL power consumption) which is expected. For an ISD of 500m a doubling of speed results to a roughly 250mW increase in the BS power consumption. The difference of BS power consumption between pedestrians (3km/h) and very high-mobility UEs (120 km/h) is highest for at the lower end of the cell size interval corresponding to an increase of 135% and 100 % for an ISD of 250m and 500m respectively. The trend of the graph by varying ISD and UE speed is similar to Fig. 10.

3) RECEIVED POWER CONSUMPTION ANALYSIS

A numerical evaluation of the average supply power consumption caused by the different HO signaling messages reception is provided in this subsection.

a: UE RECEIVED POWER CONSUMPTION

The impact of ISD and UE speed on the average supply power consumption of the UE as given by (12), is shown in Fig. 13 at a constant TTT of 32ms and an offset value of 1dB.

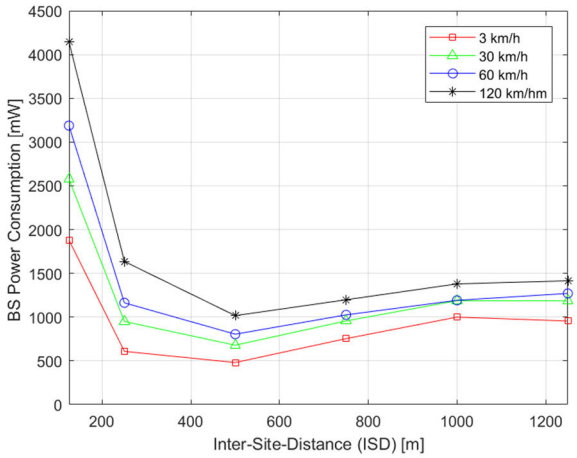

FIGURE 14. Impact of ISD and UE speed on the average supply power consumption of the BS received signaling messages, for offset = 1 dB and TTT = 32ms.

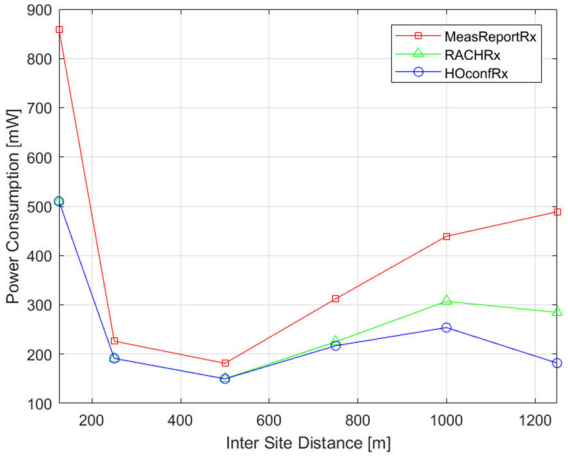

FIGURE 15. Impact of ISD on the average supply power consumption of various signaling messages reception at BS for speed = 3km/h, offset = 1 dB, and TTT = 32ms.

The signaling messages transmitted by the BS (HOcmd) are received by the UE. One observation is that the smallest simulated cell size requires that the UE received power consumption exceeds 400mW, whilst all other schemes consume less than this. With the exception of the high mobility UEs (120km/h) all other ISD and UE mobility combinations lie below 250mW.

The second observation is that UE received power consumption (for HOcmd) is higher than the transmitted power consumption (for MeasReport, RACH, and HOconf) (Fig. 10 and Fig. 13). This is attributed to two reasons. The first reason is that the required number of TBs for the HOcmd is double than the other air-interface signaling messages (see Table 2). The second cause is linked to especially the low ISDs. In our previous work [19], we found that the failures due to timer T310 expiry before HOcmd reception are very frequent when ISD is small and low when the ISD increases. We argued that for small cell sizes, the UEs that are able to transmit the measurement report subsequently move out of the serving cell coverage, and thus the HO command, sent by the serving cell, cannot reach the UE. So, the increase of UE received power consumption especially at low ISDs is linked to the HOcmd delivery failures which lead to successive signaling retransmissions. The UE speed varying trend is similar as noted in Fig. 10.

b: BS RECEIVED POWER CONSUMPTION

The impact of ISD and UE speed on the average supply power consumption of the BS as given by (12), is shown in Fig. 14 at a constant TTT and offset values. The signaling messages transmitted from the UE are received by the BS. So, the power consumption of MeasReport, RACH, and HOconf reception (BS power consumption) is much higher as compared to HOcmd reception (UE power consumption). The trend of the graph by varying ISD and UE speed is very similar to Fig. 13.

A per-type signaling power consumption breakdown for the BS is shown in Fig. 15. Noteworthy, the results are in line with Fig. 11 but the power consumption is much higher as compared to Fig. 11.

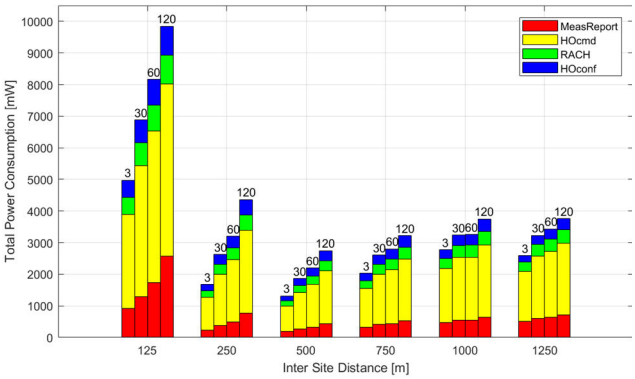

FIGURE 16. Impact of ISD and UE speed {3, 30, 60, 120} on total power consumption of each signaling message, for offset = 1 dB and TTT = 32ms.

4) TOTAL POWER CONSUMPTION ANALYSIS

Fig. 16 shows each signaling message total (including transmitted and received) power consumption during the HO procedure against various ISDs and UE speeds. It is clear from the graph that the lowest power consumption is due to HOconf and RACH messages while the highest is due to the HOcmd. This is because the number of resources (TBs) required for both transmission and reception of the HOcmd is double than the other signaling messages (see Table 2). Although the MeasReport is a major contributor to the aggregate signaling rate as per Fig. 9, the HOcmd is the major contributor to the total power consumption. Another trend in the graph shows that increasing the UE speed increases power consumption, especially at low ISDs (see 125m case). The total power consumption during HO for this case is the highest (around 5 watts at 3 km/h speed and 10 watts at 120 km/h speed) that have the worst impact on the environment as well as on the OPEX.

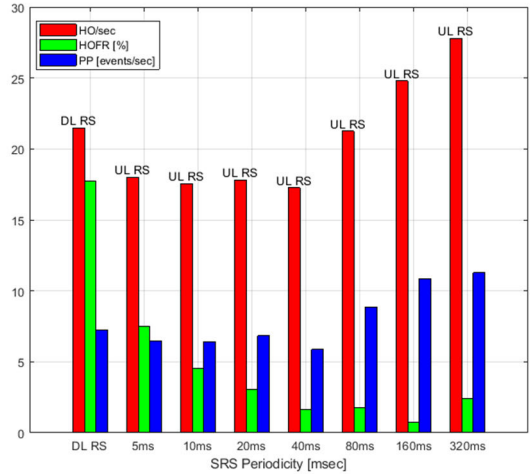

FIGURE 17. Comparison of DL and UL RS based mobility HO metrics, at fixed ISD = 500m, speed = 30km/h, DL/UL offset = 1 dB and DL/UL TTT = 32ms.

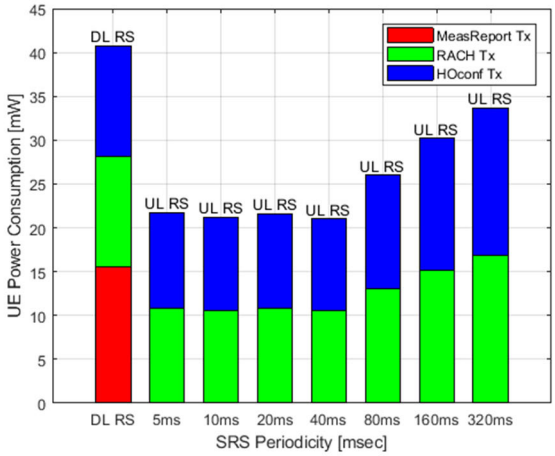

FIGURE 18. UE transmitted average supply power consumption comparison for DL and UL RS based mobility, at fixed ISD = 500m, speed = 30km/h, DL/UL offset = 1 dB and DL/UL TTT = 32ms.

B. UPLINK REFERENCE SIGNAL BASED HANDOVER RESULTS

In Section IV.A.2, we found that the optimum ISD out of the simulated cases is the ISD 500m case. Based on this finding, we fixed the ISD to 500m, and speed to 30 km/h and performed the simulations using UL RS based measurement model as explained in Section II.A. We also fixed the values of A3 UL-offset to 1dB and UL-TTT to 32 ms, the same as in DL based mobility model, to have a fair comparison. We change the SRS periodicity values to find an optimum periodicity value that reduces the power consumption during the HO procedure to its minimal level.

The impact of introducing the UL RS based mobility on the HO metrics is shown in Fig. 17. In particular, we study the HO rate, HO failure ratio (HOFR), and ping pong (PP) rate, for which detailed definitions can be found in our previous work [12]. In brief, the HO rate is measured in the total number of triggered HO events divided by the simulation time. The HOFR is defined as the total number of HO failure events divided by the total number of triggered HO events. The ping pong rate (PPR) is defined as the total number of ping pong events divided by the simulation time. A ping pong event is the occurrence of a HO between a serving cell and a target cell, followed by another HO to the original serving cell, all this happening under a predefined time. Fig. 17 shows a DL RS based HO metrics comparison with UL RS, with SRS periodicities ranging from 5 ms to 320 ms. It is clear from the graph that the SRS based model reduces the HOFR significantly in comparison to DL RS based model. This is because no measurement report transmission is required from UE to BS in case of UL RS based mobility, thus the HO procedure complete before the UE loses its connection to the s-BS. Overall, the HO rate and PP rate decrease with increasing periodicity values until a sweet spot of the SRS periodicity "40 ms" arrives. This way the UL RS based method reduces the unnecessary HOs. After the sweet spot, the HO rate and PP rate start increasing because of the high SRS periodicity values. For example, SRS is transmitted every 5ms for SRS periodicity of 5ms but every 320 ms for SRS periodicity of 320ms. High periodicity means lower SRS transmission/reception rate, i.e., the number of SRS transmission/receptions are less, increasing the gap between UL-RSRP measurements. This means that if a UE enters a poor radio link condition area (immediately after last SRS transmission), and it will remain in the same area up to 320 ms. All HO signaling will eventually not be properly transmitted/received for this period. It may also happen, that the UE failed to HO to a neighboring cell and subsequent efforts to reconnect to the same cell, resulting in a high PP rate and thus to high HO rates. It is to be noted that the ping pong events can also appear as the consequence of failed HOs to neighboring cells, and the subsequent efforts to reconnect the UE to neighboring cells even if not the most adequate at that time [19].

1) TRANSMITTED POWER CONSUMPTION COMPARISON WITH UPLINK REFERENCE SIGNAL BASED MOBILITY

In this section, we will show a detailed comparison of the power consumption when the HO related signaling messages are transmitted from the UE/BS side using DL or UL RS based mobility.

a: UE TRANSMITTED POWER CONSUMPTION

When we use the UL RS based mobility, no measurement report transmission from the UE to BS is required. Fig. 18 compares the UE DL and UL RS based average supply power consumption due to HO related signaling transmission from the UE side namely, MeasReport Tx, RACH Tx, and HOconf Tx. It is clear from the chart that the UL RS based mobility method outperforms for all SRS periodicity values, as no measurement report is transmitted for this method. The lowest UE transmitted power consumption is found for the SRS periodicity case of "40 ms", 48% lower than the DL RS based mobility case. After a 40 ms periodicity case, the UE

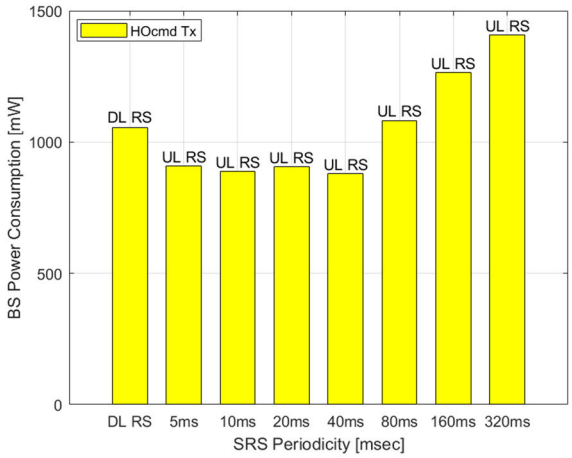

FIGURE 19. BS transmitted average supply power consumption comparison for DL and UL RS based mobility, at fixed ISD = 500m, speed = 30km/h, DL/UL offset = 1 dB and DL/UL TTT = 32ms.

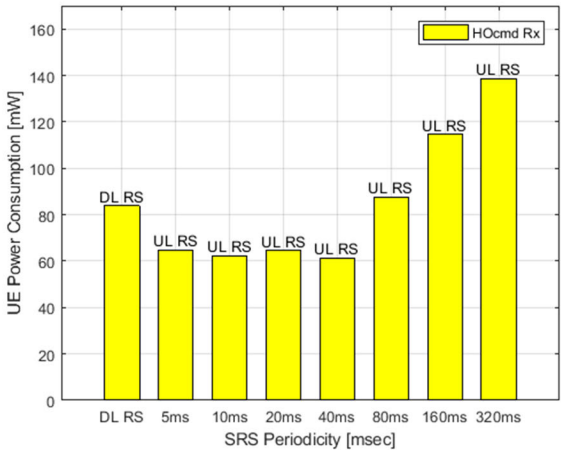

FIGURE 20. UE received average supply power consumption comparison for DL and UL RS based mobility, at fixed ISD = 500m, speed = 30km/h, DL/UL offset = 1 dB and DL/UL TTT = 32ms.

transmitted power consumption using UL RS starts increasing because of the high HO rate and PP rate we observed in Fig. 17.

b: BS TRANSMITTED POWER CONSUMPTION

Fig. 19 display a comparison of average supply BS power consumption resulting from the transmission of HO command. The BS power consumption decreases for low SRS periodicity values then it starts increasing at high periodicity values because of a high number of HO rates due to the high PP rate we observed in Fig. 17. The minimum BS transmitted power consumption is found for the SRS periodicity case of ''40 ms'', almost 17% lower than the DL RS based mobility method.

2) RECEIVED POWER CONSUMPTION COMPARISON WITH UPLINK REFERENCE SIGNAL BASED MOBILITY

In this section, we will show a detailed comparison of the power consumption when the HO related signaling messages are received at the UE/BS side using DL or UL RS based mobility. It is to be noted that the HO signaling messages that are transmitted from the UE side are received at the BS and similarly the messages transmitted from the BS side are received at UE.

a: UE RECEIVED POWER CONSUMPTION

Fig. 20 exhibits a comparison of average supply UE power consumption resulting from the reception of HO command and it follows the same trend as we noted in Fig. 17. The smallest UE received power consumption is found for the SRS periodicity case of ''40 ms'', almost 27% lower than the DL RS based mobility case.

b: BS RECEIVED POWER CONSUMPTION

The HO related messages transmitted from the UE side are received at the BS. Using the UL RS based mobility, no measurement report is transmitted from the UE thus there is

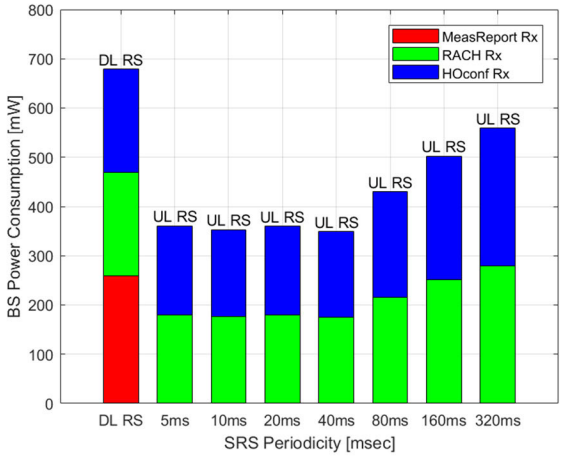

FIGURE 21. BS received average supply power consumption comparison for DL and UL RS based mobility, at fixed ISD = 500m, speed = 30km/h, DL/UL offset = 1 dB and DL/UL TTT = 32ms.

no power consumption at the BS side due to this signaling message. Fig. 21 convey the BS DL and UL RS based average supply power consumption due to HO related signaling reception. It is understandable from the graph that the UL RS based mobility method outperforms for all SRS periodicity values, as no measurement report is received for this case. The lowest BS power consumption is found for the SRS periodicity case of ''40 ms'', which is practically half (49%) of the DL RS based mobility case.

3) REFERENCE SIGNAL TRANSMISSION AND MEASUREMENT POWER CONSUMPTION

In this section, we compare the power consumption due to DL RS and UL RS transmission and measurement at UE/BS side. For DL RS transmission/measurement, we assumed that one RE is required for one RSRP measurement, and for average RSRP, we take the average over eight REs [38]. So the resources consumed for one RSRP measurement are eight REs for DL based mobility. To measure the eight strongest

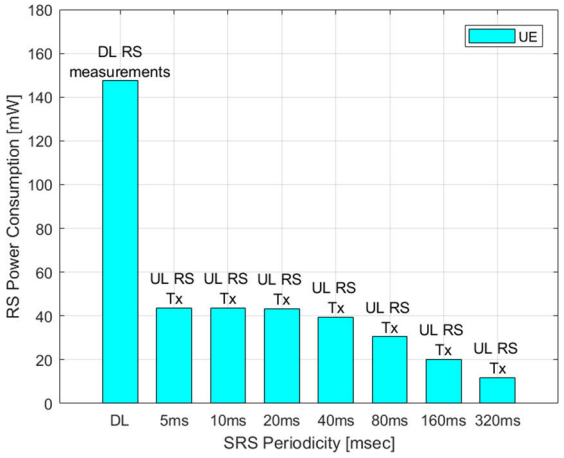

FIGURE 22. UE reference signal average supply power consumption comparison for DL and UL RS based mobility, at fixed ISD = 500m, speed = 30km/h, DL/UL offset = 1 dB and DL/UL TTT = 32ms.

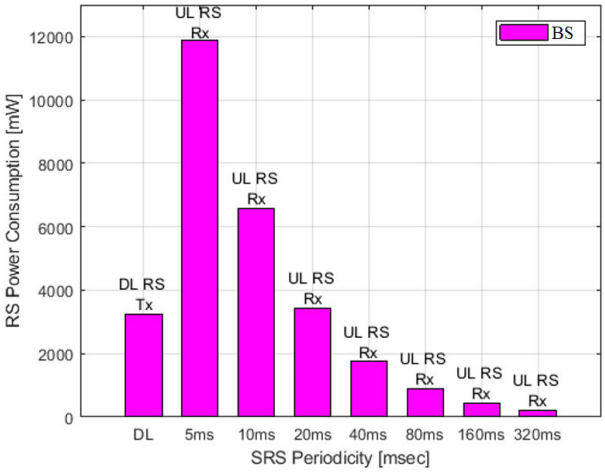

FIGURE 23. BS reference signal average supply power consumption comparison for DL and UL RS based mobility, at fixed ISD = 500m, speed = 30km/h, DL/UL offset = 1 dB and DL/UL TTT = 32ms.

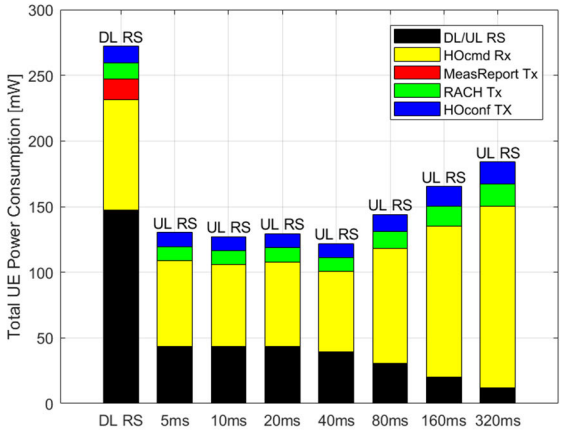

FIGURE 24. Total UE average supply power consumption comparison for DL and UL RS based mobility, at fixed ISD = 500m, speed = 30km/h, DL/UL offset = 1 dB and DL/UL TTT = 32ms.

cells for each UE, we use sixty-four REs. Then, we use (8) and (12) to find DL RS transmitted and measurement/received power consumption respectively. Similarly, we use $(N_{sc}^{RB} \times B_{SRS})/K_{TC}$ REs for each SRS transmission/reception. Then, we use (8) and (12) to find UL RS transmitted and measurement power consumption respectively. The signaling rate for the DL based RSRP and the UL-RSRP measurements are obtained using the system-level simulator.

Fig. 22 shows the average supply UE power consumption for DL RS measurements in comparison to UL RS transmission power consumption. It is to be noted that the DL RSs are received at UE while the UL RSs are transmitted from the UE. It is visible from the graph that the DL RS measurements consume a lot of the UE power while the UL RS has the lowest UE power consumption. This is because the UE has to measure the DL RS from both the s-BS as well as the t-BSs that result in high power consumption while in the case of SRS, UE only needs to send the SRS that is received at multiple BSs. The SRS transmission power consumption at the UE practically remains consistent between 5ms and 20ms. Also, as the SRS periodicity increase, the UL RS power consumption reduces because of less number of UL RS transmissions. For the ''40ms'' periodicity case, the UL RS method consumes almost four times less UE power in comparison to DL based method.

The DL RSs are transmitted from the BS side while the UL RS measurements are processed at the BS. Fig. 23 presents the average supply BS power consumption for DL RS transmission in comparison to UL RS measurement power consumption. For low periodicity values {5ms, 10ms, 20ms}, the power consumption of SRS measurements is higher than the DL RS transmission because of the high number of SRS reception at multiple BSs. It is to be noted that the UL RS transmitted from the UE is received at multiple BSs within the UL RS transmission range. As the SRS periodicity increase, the number of SRS transmissions reduces as noted in Fig. 22 that further reduces the SRS measurement power consumption. For the ''40ms'' periodicity case, the UL RS method consumes half of the BS power in comparison to DL based method.

4) TOTAL POWER CONSUMPTION COMPARISON

In this section, we show the total average supply power consumption for each air-interface HO related signaling message (the sum of transmitted and received power consumption) to find an optimum periodicity value. The total UE average supply power consumption is shown in Fig. 24 and the total BS average supply power consumption in Fig. 25 including the DL/UL RS power consumption. From the UE perspective, the proposed UL-HO scheme is more attractive since it reduces the overall UE power spent during HO by avoiding the measurement report transmission for all periodicity cases (see Fig. 24). From the BS perspective, at periodicity 5ms and 10ms cases, the UL-HO procedure requires a high amount of power in comparison to DL RS based HO, since the BS has to process UL RSs very often as compared to the DL-HO case. This trend changes for other all periodicity cases where the

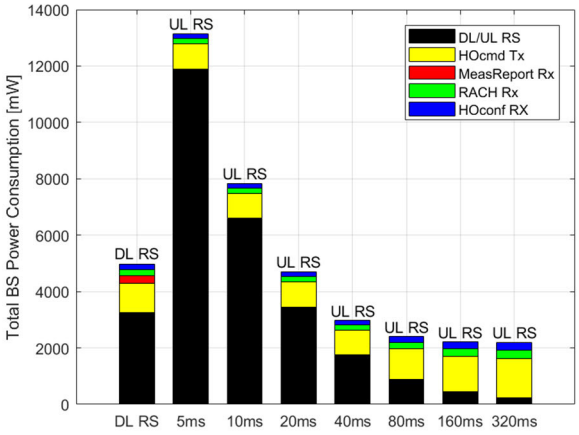

FIGURE 25. Total BS average supply power consumption comparison for DL and UL RS based mobility, at fixed ISD = 500m, speed = 30km/h, DL/UL offset = 1 dB and DL/UL TTT = 32ms.

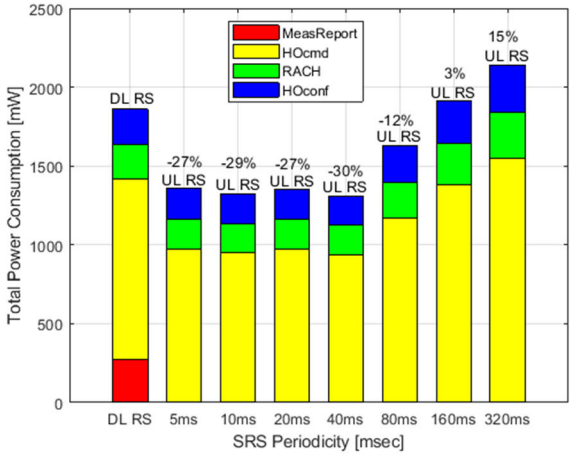

FIGURE 26. Total average supply power consumption comparison for DL and UL RS based mobility, at fixed ISD = 500m, speed = 30km/h, DL/UL offset = 1 dB and DL/UL TTT = 32ms.

UL RS based HO scheme outperforms the DL RS based HO procedure in terms of total BS power consumption. The total power consumption is shown in Fig. 26 where the percentage of power increase or decrease in comparison to DL RS based mobility is also shown without considering RS power consumption. The plot presents that the total power consumption shows a decreasing trend in comparison to DL based mobility until a sweet-spot of 40ms SRS periodicity case arrives, then it again starts increasing. After the 40ms periodicity case, the high power consumption is due to frequent HOs we noted in Fig. 17. The lowest total average supply power consumption is found for the SRS periodicity case of "40 ms", 30% lower than the DL RS based mobility case.

V. CONCLUSION

In this work, a simulation analysis is performed for the signaling overheads and the power consumption due to the HO procedure when different UE speeds and cell sizes are applied. In the DL based mobility case, we observe that the largest contributor to air-interface signaling overhead is the MeasReport transmission within the HO procedure. We also note that the total power consumption of the MeasReport is higher than the RACH and HOconf messages. The results show that, for our considered setup, an optimum cell size (ISD = 500m out of simulated cases) can be found around which any increase or decrease of the cell size brings the performance degradation in terms of higher signaling rate and the higher power consumption. These results are in complete accordance with the UL transmission limitations as noted in our previous work [19]. We assess that increasing the UE speed degrades the performance, significantly for small ISDs, as expected.

Based on the optimum ISD we utilize the UL RS based method to make the measurement procedure more power-efficient (because no measurement report transmission is required using this method). The numerical results show that the proposed UL RS based method reduces the average supply power consumption, UE transmitted by 48%, BS transmitted by 17%, UE received 27%, BS received 49% and total power consumption during the HO procedure by 30% in comparison to downlink RS based method, for an optimum SRS periodicity case of "40 ms". We found that the UL RS transmission requires almost four times less power consumption while the UL RS measurement only half of the power consumption in comparison to the downlink RS based method. The proposed method is power-efficient at both UE and BS side and it is beneficial since it reduces the OPEX and the environmental effects. It is also an excellent candidate of an energy-efficient HO procedure in future releases of the 3GPP standards heading towards denser network deployments and higher frequencies. In the future, we will propose a UE specific SRS periodicity selection procedure (e.g. as a function of speed) to improve the network performance and further reduce the power consumption. It may be also interesting to propose an SRS power control procedure to assign the SRS power according to, not only the s-BS, but so the UL RS can be received at some target number of neighboring BSs.

REFERENCES

[1] *Worldwide Mobile Cellular Subscribers to Reach 4 Billion Mark Late 2008*, International Telecommunication Union, Geneva, Switzerland, 2008.

[2] Y. Song, P.-Y. Kong, and Y. Han, "Potential of network energy saving through handover in HetNets," *IEEE Trans. Veh. Technol.*, vol. 65, no. 12, pp. 10198–10204, Dec. 2016.

[3] K. Kanwal, "Increased energy efficiency in LTE networks through reduced early handover," Ph.D. dissertation, Dept. Comput. Sci. Technol., Univ. Bedfordshire, Bedford, U.K., 2017.

[4] L. G. Giordano, L. Campanalonga, D. Lopez-Perez, A. Garcia-Rodriguez, G. Geraci, P. Baracca, and M. Magarini, "Uplink sounding reference signal coordination to combat pilot contamination in 5G massive MIMO," in *Proc. IEEE Wireless Commun. Netw. Conf. (WCNC)*, Apr. 2018, pp. 1–6.

[5] X. Gelabert, C. Qvarfordt, M. Costa, P. Kela, and K. Leppanen, "Uplink reference signals enabling user-transparent mobility in ultra dense networks," in *Proc. IEEE 27th Annu. Int. Symp. Pers., Indoor, Mobile Radio Commun. (PIMRC)*, Sep. 2016, pp. 1–6.

[6] M. S. Mushtaq, S. Fowler, and A. Mellouk, "Power saving model for mobile device and virtual base station in the 5G era," in *Proc. IEEE Int. Conf. Commun. (ICC)*, May 2017, pp. 1–6.

[7] H. Holtkamp, G. Auer, V. Giannini, and H. Haas, "A parameterized base station power model," *IEEE Commun. Lett.*, vol. 17, no. 11, pp. 2033–2035, Nov. 2013.
[8] M. Lauridsen, L. Noël, T. B. Sørensen, and P. Mogensen, "An empirical LTE smartphone power model with a view to energy efficiency evolution," *Intel Technol. J.*, vol. 18, no. 1, pp. 172–193, Mar. 2014.
[9] A. Ibrahim, K. Kpochi, and E. Smith, "Energy Consumption Assessment of Mobile Cellular Networks," *Amer. J. Eng. Res.*, vol. 7, no. 3, pp. 96–101, 2018.
[10] M. M. A. Hossain, K. Koufos, and R. Jantti, "Minimum-energy power and rate control for fair scheduling in the cellular downlink under flow level delay constraint," *IEEE Trans. Wireless Commun.*, vol. 12, no. 7, pp. 3253–3263, Jul. 2013.
[11] M. Höyhtyä, O. Apilo, and M. Lasanen, "Energy consumption analysis of D2D communication in 5G systems: Latest advances in 3GPP standardization," *Future Internet MDPI J.*, vol. 10, no. 3, pp. 1–18, 2018.
[12] M. Haris, S. Jangsher, H. K. Qureshi, S. Mumtaz, and A. A. Dulaimi, "Power allocation for reliable smart grid communication employing neighborhood area networks," in *Proc. IEEE Global Commun. Conf. (GLOBECOM)*, Dec. 2018, pp. 1–6.
[13] Y. He, L. Tang, Z. Zhou, S. Mumtaz, K. M. S. Huq, and J. Rodriguez, "Two time-scale resource allocation in hybrid energy powering 5G wireless system," in *Proc. IEEE Global Commun. Conf. (GLOBECOM)*, Waikoloa, HI, USA, Dec. 2019, pp. 1–6.
[14] M. T. Nguyen, S. Kwon, and H. Kim, "Mobility robustness optimization for handover failure reduction in LTE small-cell networks," *IEEE Trans. Veh. Technol.*, vol. 67, no. 5, pp. 4672–4676, May 2018.
[15] K. Kanwal and G. A. Safdar, "Energy efficiency and superlative TTT for equitable RLF and ping pong in LTE networks," *Mobile Netw. Appl.*, vol. 23, no. 6, pp. 1682–1692, Dec. 2018.
[16] E. Demarchou, C. Psomas, and I. Krikidis, "Mobility management in ultra-dense networks: Handover skipping techniques," *IEEE Access*, vol. 6, pp. 11921–11930, 2018.
[17] R. Arshad, H. Elsawy, S. Sorour, T. Y. Al-Naffouri, and M.-S. Alouini, "Handover management in 5G and beyond: A topology aware skipping approach," *IEEE Access*, vol. 4, pp. 9073–9081, Dec. 2016.
[18] A. Mukherjee, "Energy efficiency and delay in 5G ultra-reliable low-latency communications system architectures," *IEEE Netw.*, vol. 32, no. 2, pp. 55–61, Mar. 2018.
[19] M. Tayyab, G. P. Koudouridis, and X. Gelabert, "A simulation study on LTE handover and the impact of cell size," in *Proc. Int. Conf. Broadband Commun.*, 2018, pp. 398–408.
[20] M. Tayyab, G. P. Koudouridis, X. Gelabert, and R. Jantti, "Signaling overhead and power consumption during handover in LTE," in *Proc. IEEE Wireless Commun. Netw. Conf. (WCNC)*, Apr. 2019, pp. 1–6.
[21] M. Tayyab, G. P. Koudouridis, X. Gelabert, and R. Jantti, "Receiver power consumption during handover in LTE," in *Proc. IEEE 2nd 5G World Forum (5GWF)*, Sep. 2019, pp. 74–79.
[22] H. Lundqvist, G. P. Koudouridis, and X. Gelabert, "Joint tracking of groups of users with uplink reference signals," in *Proc. IEEE 22nd Int. Workshop Comput. Aided Model. Des. Commun. Links Netw. (CAMAD)*, Jun. 2017, pp. 1–5.
[23] M. Koivisto, M. Costa, J. Werner, K. Heiska, J. Talvitie, K. Leppanen, V. Koivunen, and M. Valkama, "Joint device positioning and clock synchronization in 5G ultra-dense networks," *IEEE Trans. Wireless Commun.*, vol. 16, no. 5, pp. 2866–2881, May 2017.
[24] H. Xu, X. Wang, W. Liu, and W. Shao, "An uplink based mobility management scheme for 5G wireless network," in *Proc. ICC - IEEE Int. Conf. Commun. (ICC)*, May 2019, pp. 1–6.
[25] *Comparative Power Analysis Between UL and DL-based Mobility*, document TSG-RAN WG1, 3GPP, Oct. 2016.
[26] *UL Mobility in Connected Active Mode* document TSG-RAN WG1, 3GPP, Feb. 2017.
[27] J. Zhang, L. Lu, Y. Sun, Y. Chen, J. Liang, J. Liu, H. Yang, S. Xing, Y. Wu, J. Ma, I. B. F. Murias, and F. J. L. Hernando, "PoC of SCMA-based uplink grant-free transmission in UCNC for 5G," *IEEE J. Sel. Areas Commun.*, vol. 35, no. 6, pp. 1353–1362, Jun. 2017.
[28] M. Tayyab, X. Gelabert, and R. Jantti, "A survey on handover management: From LTE to NR," *IEEE Access*, vol. 7, pp. 118907–118930, 2019.
[29] (Feb. 2020). *O-RAN-WG1-O-RAN Architecture Description v1.0*. [Online]. Available: https://www.o-ran.org/specifications
[30] *E-UTRA and E-UTRAN; Overall description; Stage 2 (Release 15)*, document TS 36.300, 3GPP, Dec. 2017.
[31] *NR; NR and NG-RAN Overall Description; Stage 2 (Release 15)*, document TS 38.300, 3GPP, Mar. 2019.
[32] X. Gelabert, G. Zhou, and P. Legg, "Mobility performance and suitability of macro cell power-off in LTE dense small cell HetNets," in *Proc. IEEE 18th Int. Workshop Comput. Aided Model. Design Commun. Links Netw. (CAMAD)*, Sep. 2013, pp. 99–103.
[33] J. Peisa, "5G Evolution: 3GPP Releases 16 & 17 Overview," *Ericsson Technol. Rev.*, vol. 9, pp. 1–5, Mar. 2020.
[34] *Further Advancements for E-UTRA Physical Layer Aspects (Release 9)*, document TR 36.814, 3GPP, Mar. 2010.
[35] *E-UTRA Radio Resource Control (RRC); Protocol specification (Release 9)*, document TS 36.331, 3GPP, Mar. 2010.
[36] *Requirements for Support of Radio Resource Management (Release 9)*, document TS 36.133, 3GPP, Mar. 2013.
[37] C. Desse, "Flexible power modeling of LTE base stations," in *Proc. IEEE Wireless Commun. Netw. Conf. (WCNC)*, Dec. 2012, pp. 62–2858.
[38] *Physical Channels and Modulation (Release 15)*, document TS 36.211, 3GPP, Mar. 2018.
[39] *Physical Channels and Modulation (Release 16)*, document TS 38.211, 3GPP, Mar. 2020.
[40] *Evolved Universal Terrestrial Radio Access (E-UTRA); Physical layer procedures*, document TS 36.213, 3GPP, Mar. 2018.
[41] *Handover Performance in a Manhattan Scenario*, document 3. R1-091791, May 2009.
[42] S. Sesia, I. Toufik, and M. Baker, *LTE—The UMTS Long Term Evolution: From Theory to Practice*. Hoboken, NJ, USA: Wiley, 2011.
[43] J. Rodriguez, "SECRET—Secure network coding for reduced energy next generation mobile small cells," in *Proc. IEEE Internet Technol. Appl. (ITA) Conf.*, Dec. 2017, pp. 329–333.

MUHAMMAD TAYYAB received the B.Sc. degree from the University of the Punjab, Lahore, Pakistan, in 2012, and the M.Sc. degree (Hons.) from the King Fahd University of Petroleum and Minerals (KFUPM), Saudi Arabia, in 2017, both in electrical engineering. He is currently pursuing the Ph.D. degree in electrical engineering with Aalto University, Finland. From 2013 to 2015, he gained more than two years of professional experience as an RF Planning and Optimization Executive at Wi-Tribe Pakistan Ltd. (Ooredoo Group). During his stay at KFUPM, he was associated with the King Abdullah University of Science and Technology (KAUST), Saudi Arabia, as a Visiting Student, and also with the KFUPM-KAUST Joint Research Initiative. He has been a Researcher with the Helsinki Research Center, Huawei Technologies Finland Oy, since February 2018. His current research interests include energy-efficient mobility for small-cell overlaid cellular networks. He received the Gold Medal Award for obtaining the first position in the B.Sc. degree.

GEORGE P. KOUDOURIDIS received the B.S. degree in computer sciences from the Department of Computer and Systems Sciences, Stockholm University (SU), Stockholm, Sweden, in 1995, and the Ph.D. degree in electrical engineering on telecommunications from the Royal Institute of Technology (KTH), Stockholm, in 2016. In 2008, he was with Telia Research and TeliaSonera Mobile R&D. He is currently a Principal Researcher at the Radio Access Network Systems Lab, Huawei Technologies Sweden AB, Kista, Sweden. His research interests include radio resource management, spectrum allocation, self-organized networks, and machine learning-based optimization in wireless networks.

XAVIER GELABERT received the M.S. degree in electrical engineering from the Royal Institute of Technology (KTH), in 2003, and the M.S. degree in telecommunication engineering and the Ph.D. degree from the Technical University of Catalonia (UPC), in 2004 and 2010, respectively. Since 2012, he has been a Senior Research Engineer with the Huawei Stockholm Research Centre. He has more than 15 years of research experience across academia (UPC, GATech, and KCL), a research institute (iTEAM), a telco operator (Orange Labs), and an equipment vendor (Huawei). His research interests include radio and spectrum resource management, self-organized networks, and more recently baseband systems implementation and design. He actively contributed to 3GPP NR in RAN1 and RAN2 and holds a number of related patents.

RIKU JÄNTTI (Senior Member, IEEE) received the M.Sc. degree (with distinction) in electrical engineering and the D.Sc. degree (with distinction) in automation and systems technology from the Helsinki University of Technology (TKK), in 1997 and 2001, respectively. He is currently a Professor in communications engineering and the Head of the Department of Communications and Networking, Aalto University School of Electrical Engineering, Finland. Prior to joining Aalto (formerly known as TKK) in August 2006, he was the Professor pro tem with the Department of Computer Science, University of Vaasa. His research interests include radio resource control, spectrum management, and performance optimization of wireless communication systems. He is an Associate Editor of the IEEE TRANSACTIONS ON VEHICULAR TECHNOLOGY.